Journal of Catalysis 285 (2012) 115–123

Contents lists available at SciVerse ScienceDirect

Journal of Catalysis

journal homepage: www.elsevier.com/locate/jcat

Kinetics and mechanism of olefin methylation reactions on zeolites

Ian M. Hill [a], Saleh Al Hashimi [b], Aditya Bhan [a,*]

[a] Department of Chemical Engineering and Materials Science, University of Minnesota – Twin Cities, 421 Washington Avenue SE, Minneapolis, MN 55455, USA
[b] Department of Chemical Engineering, The Petroleum Institute, P.O. Box 2533, Abu Dhabi, United Arab Emirates

ARTICLE INFO

Article history:
Received 10 May 2011
Revised 5 August 2011
Accepted 19 September 2011
Available online 20 October 2011

Keywords:
Methanol-to-gasoline conversion
Zeolites
Shape selectivity
Hydrocarbon pool
Surface methoxide groups
Alkylation
Olefin methylation
Brønsted acid catalysis

ABSTRACT

Ethylene and propylene methylation rates increased linearly with olefin pressure but did not depend on dimethyl ether (DME) pressures on proton-form FER, MFI, MOR, and BEA zeolites at low conversions (<0.2%) and high DME/olefin ratios (30:1) in accordance with a mechanism that involves the zeolite surface being predominantly covered by DME-derived species reacting with olefins. Higher first-order reaction rate constants for both ethylene and propylene methylation were observed over H-BEA and H-MFI compared with H-FER and H-MOR, indicating that olefin methylation reaction cycles involved in the conversion of methanol-to-gasoline over zeolitic acids are propagated to varying extents by different framework materials. Systematically lower activation barriers and higher rate constants were observed for propylene methylation in comparison with ethylene methylation over all frameworks studied, reflecting the increased stability of reaction intermediates and activated complexes with increasing olefin substitution. A binomial distribution of $d_0/d_3/d_6$ in unreacted DME upon introduction of equimolar protium- and deuterium-form DME under steady-state reaction conditions of ethylene methylation over H-MFI suggests the presence and facile formation of reactive surface-bound methoxide species and the absence of C–H bond cleavage.

1. Introduction

Processing synthetic fuels and commodity chemical precursors from alternative carbon sources is a necessity in light of the depletion of global petroleum reserves. A methanol-based platform has become a dedicated topic of research as it is readily synthesized via the catalytic conversion of synthesis gas [1,2], which is formed through the oxidative conversion of a variety of carbon-based feedstocks (including coal [3,4], natural gas [5], and biomass [6,7]). Acid-catalyzed conversion of methanol-to-hydrocarbons (MTH) can be used to produce hydrocarbons in the gasoline range [8–22], aromatics [23–25], and light olefins [26–30] starting from either methanol or dimethyl ether (DME) although typically not with high selectivity [10,31–33].

There has been much debate over the past 30 years regarding two aspects of the MTH reaction: the origin of the first C–C bond from the C_1 reactants and the mechanism by which the MTH reaction propagates. A broad consensus has emerged in the recent literature concerning the inability of zeolite-adsorbed C_1 species to couple directly into hydrocarbons at rates relevant for steady-state MTH catalysis. The presence of persistent surface-bound C_1 methoxide species in zeolites has been described by Wang and Hunger using infrared spectroscopy and ^{13}C MAS NMR studies [34]. Waroquier et al. [35–37] have shown, through a series of theoretical studies, that energy barriers for C–H bond activation on surface-bound methoxide species are prohibitively large (242 kJ mol^{-1}) compared to indirect mechanistic routes involving the methylation of unsaturated hydrocarbons (<94 kJ mol^{-1}) [18,25]. Isotopic distributions in product olefins in the ^{13}C-methanol methylation of aromatics have shown that all ethene and majority propene are formed through the cracking of arenes on H-ZSM-5, H-MOR, and H-BEA catalysts, and not direct coupling of C_1 species [25]. Experiments have also shown that the catalyst induction period is sensitive to hydrocarbon impurity concentrations in methanol [17,18]. These results show that over zeolite and zeotype catalysts, the methylation of unsaturated hydrocarbons proceeds in the absence of direct ethylene formation from methanol coupling. Haw et al. [38] report a binomial distribution of unlabeled/tri-labeled/hexa-labeled dimethyl ether in the product stream using a 1:1 mixture of unlabeled and d_6 dimethyl ether on SAPO-34 at 523 K clearly demonstrating the activation of C–O bonds, but no C–H bond cleavage as would be necessary in the formation of direct C_1 coupling products.

An early reaction mechanism for MTH outlined by Dessau and LaPierre [13,39] entails: (i) methylation of olefinic species to form higher homologs, (ii) formation of arenes and alkanes through hydrogen transfer steps, (iii) methylation of arenes to form methylbenzenes, and (iv) cracking reactions that form smaller olefinic

* Corresponding author.
E-mail addresses: hill0651@umn.edu (I.M. Hill), salhashimi@pi.ac.ae (S.A. Hashimi), abhan@umn.edu (A. Bhan).

0021-9517/$ - see front matter © 2011 Elsevier Inc. All rights reserved.
doi:10.1016/j.jcat.2011.09.018

species. Later work from Dahl and Kolboe stressed the importance of a co-catalytic "hydrocarbon pool," consisting of entrained organic species within the zeolite framework that act as a methylation and cracking center and are responsible for the generation of ethylene and propylene in the observed MTH product distribution [11,12,40]. Several theoretical and isotopic labeling studies have confirmed the importance of this indirect hydrocarbon pool mechanism [11,12,14,15,17,25,30,40–47].

Extensive theoretical and experimental studies have focused on the role of entrained aromatic compounds—mainly polymethylbenzenes, as naphthenic species were calculated to have too high an energy barrier to compete over CHA frameworks using ONIOM-derived energies and geometries (170 kJ mol^{-1} compared to 129 kJ mol^{-1}) [24]—as potential hydrocarbon pool organic co-catalysts. The gem-methylation of a methylbenzene species allows for one of three events to occur: (i) the elimination of the geminal hydrogen to complete the methyl substitution, (ii) elimination of a methyl hydrogen to allow for side-chain methylation (side-chain mechanism) [30,48], or (iii) the collapse from a 6-membered to a 5-membered ring, generating a branched alkyl substituent (paring mechanism) [15,43,49]. These alkyl groups are then susceptible to cracking, forming the observed C_2–C_4 olefins in the product distribution and occluded lower methylbenzenes. The predominant occluded polymethylbenzenes and their methylated cation intermediates have also been directly observed using *in situ* ^{13}C MAS NMR [43] and GCMS analysis of the hydrocarbon pool via HF digestion of the reacted zeolite/zeotype catalyst [43,49]. These studies have shown that large-pore zeolites and zeotype materials (like H-BEA and H-SAPO-34) operate via an aromatic hydrocarbon pool consisting mostly of pentamethylbenzene and hexamethylbenzene while di-, tri-, and tetra-methylbenzenes dominate the aromatic hydrocarbon pool of medium-pore H-ZSM-5 [43,49].

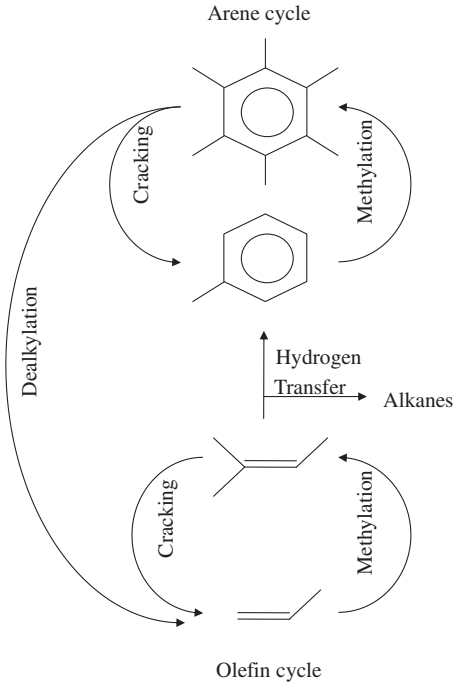

Scheme 1. Dual olefin and arene methylation cycle that comprises the hydrocarbon pool mechanism for MTH on zeolite catalysts. Successive methylation steps upgrade olefins to higher homologs, which may crack or generate arenes and alkanes via hydrogen transfer steps. These arenes are successively methylated to form higher methylbenzenes and subsequently eliminate alkyl groups to form lower polymethylbenzenes (PMBs) and light olefins.

Recently, computational [50–52] and experimental [28,29,53] studies have begun to focus on the viability and reactivity of an olefin hydrocarbon pool. The kinetic induction period observed and the inability to explain the primary product selectivity in MTH catalysis led several researchers early on to propose that a relatively inefficient mechanism leads to the formation of first C–C bond followed by olefin chain growth and cracking [13]. Chen and Reagan [54] initially reported the autocatalytic effect of olefinic compounds in MTH. Langner [55] noted that co-feeding a small amount of higher alcohols led to an 18-fold reduction in the induction period. These initial studies all point to a catalytic role for olefin methylation where an existing olefin molecule is repeatedly methylated by methanol to form higher homologs. Lesthaeghe et al. [50] have shown through van der Waals corrected ONIOM calculations over 48T zeolite clusters that the energy barriers for olefin methylation are of similar magnitude (60–80 kJ mol^{-1}) to those for methylation of lower methylbenzenes in H-ZSM-5, thereby suggesting that contribution of the alkene hydrocarbon pool toward the observed product distribution is significant. A simplified reaction scheme for a "dual-cycle" mechanism is shown below (Scheme 1); the two hydrocarbon pools undergo interconversion on H-ZSM-5 as demonstrated in recent isotopic studies by Kolboe et al. [25,56], where the authors show that 25–50% of the carbon in product ethylene and propylene originate from co-fed toluene in the presence of ^{13}C methanol, implying that ethylene and propylene are formed primarily from dealkylation reactions of arene species.

Through the selective operation of one cycle of the dual-cycle mechanism, the product selectivity of MTH chemistry can be systematically controlled. The arene methylation cycle is largely suppressed over H-ZSM-22 (a one-dimensional 10-membered ring channel zeolite) because arene methylation is limited by sterics to a larger extent than olefin methylation [28,29,41,57]. In this special case, propylene and higher-order olefins, which are the major products of the olefin cycle, are selectively produced over ethylene and alkanes/arenes, which arise from the formation and dealkylation of arenes [41]. The complex role that the dual olefin–arene methylation cycle plays in the observed catalytic rate and selectivity for MTH implies that it is difficult to isolate one hydrocarbon pool cycle over another. Reduced methylation barriers with increasing olefin chain length, the subsequent isomerization of hydrocarbon products, and formation of olefinic species from both methylation and cracking reactions at conversions relevant for practice of MTH make quantitative evaluation of kinetic parameters of olefin methylation on zeolites experimentally challenging. The difficulty in isolating kinetically-relevant steps is evidenced by the sparse reporting of reaction rates and kinetic parameters for MTH reactions [9,26,27,52].

In this work, methylation kinetics of ethylene and propylene were measured on proton-form MFI, MOR, BEA, and FER zeolites at low olefin conversions (<0.2%) and high DME/olefin ratios (15–60:1). We report that the kinetics of olefin methylation are consistent with a mechanism involving a surface predominantly covered by DME-derived species (zero-order kinetics) that react with olefinic species in kinetically-relevant steps (first-order kinetics). A systematic decrease in activation barriers was noted with increasing substitution of the olefin. These data show that MFI, MOR, BEA, and FER zeolites propagate the olefin methylation cycle to varying extents and thereby explain the marked diversity in selectivity and yield for C_1 homologation using different zeolites.

The identity of the reactive C_1 surface species on the zeolitic Al site responsible for the methylation of olefins and arenes determines the MTH reaction behavior under varying operating conditions. The reactant state for olefin methylation is explained either as a surface methyl group reacting with a gas-phase olefin [34], or through the formation of a methanol/olefin co-adsorbed complex

[51,58,59]. This report aims to elucidate the nature of the methylating surface species on zeolites via experimental evidence and energetic arguments in an effort to complete the mechanistic picture of the olefin methylation reaction cycle in MTH.

2. Materials and methods

2.1. Catalyst preparation

FER, MFI, MOR, and BEA zeolite samples (silicon-to-aluminum ratios were determined by ICP-OES elemental analysis performed at Galbraith Laboratories, and further characterization is included in the Supplemental information section) from Zeolyst were sieved in their NH_4^+ form to obtain aggregate particle sizes between 180 and 425 μm (40–80 mesh). Treatment in dry air (1.67 $cm^3\ s^{-1}$ NTP, ultrapure, Minneapolis Oxygen) during a 0.0167 K s^{-1} temperature ramps to 773 K and holding for 4 h thermally decomposed NH_4^+ to H^+ and $NH_{3(g)}$. Protonated zeolite samples used in this study are denoted as H-FER, H-MFI, H-MOR, and H-BEA. Chiang and Bhan [60] performed DME titration experiments of zeolite acid sites over all of the samples used in this study and have shown that 0.5 ± 0.08 DME molecules are adsorbed per acid site. From this information, we conclude that the Brønsted acid site concentration in these samples is nearly identical to the aluminum concentration determined by ICP-OES, which also excludes the presence of a significant fraction of Lewis acidic aluminum centers in these framework materials [60].

2.2. Steady-state catalytic reactions of DME and light olefins

Steady-state olefin methylation reactions were carried out in a 9.52-mm OD packed-bed stainless steel tube reactor at atmospheric pressure and differential conversions (<0.2%). Catalyst samples (0.005–0.260 g) were supported between quartz wool plugs under isothermal conditions using a furnace (National Element Furnace FA120 type) regulated by a Watlow Temperature Controller (96 Series). Catalyst temperature was monitored using a K-type thermocouple threaded through a coaxial thermal well penetrating the catalyst bed. Samples were treated in flowing He (1.67 $cm^3\ s^{-1}$, ultrapure, Minneapolis Oxygen) at 773 K (0.0334 K s^{-1} temperature ramp) for 4 h prior to cooling to reaction temperatures (353–473 K). A mixture of dimethyl ether (DME), argon, and methane (50:49:1; Praxair certified standard grade) (0.26–0.62 bar) was combined with a C_2H_4 (Matheson Tri-Gas, chemical purity grade) or C_3H_6 (50:50 mixture with argon; Praxair certified standard grade) (0.005–0.03 bar) stream and He to maintain a total flow rate of 1.67 $cm^3\ s^{-1}$ (WHSV = 6.4–335 $cm^3\ g^{-1}\ s^{-1}$). Reaction order dependencies were determined by varying either DME or olefin flow rates in the feed stream while keeping the other constant and adjusting He flow to compensate for the change in overall reactant flow rate. Reactor effluent composition was monitored via gas chromatography (Agilent 7890) through a methyl-siloxane capillary column (HP-1, 50.0 m × 320 μm × 0.52 μm) connected to a flame ionization detector and a packed column (Supelco HAYSEP DB packed column, 12 ft) connected to a thermal conductivity detector.

2.3. Introduction of d_6-DME in ethylene methylation reactions on H-MFI

Isotopic experiments were performed on the experimental setup described above. A 0.42 $cm^3\ s^{-1}$ total flow of ethylene (0.03 bar) and a mixture of 50:49:1 DME/Ar/CH_4 (0.67 bar) with balance helium was passed over 100 mg of H-MFI for 4.6 h at 393 K. At steady-state reaction conditions, DME pressure was reduced to 0.17 bar, and 0.15 bar d_6 DME (Isotec, 99.9 at.% isotopic purity) was introduced into the reaction system. Product mass distributions were monitored using an online mass spectrometer (MKS Cirrus 200 Quadrupole mass spectrometer system), and ethylene methylation rates were monitored using gas chromatographic protocols described above.

3. Results and discussion

3.1. Ethylene methylation

Steady-state ethylene methylation reactions were run at differential conversions (<0.2%) to maintain low propylene concentrations, inhibiting secondary and further reactions. Fig. 1 shows that every zeolite probed in this study obeys a first-order dependence of the propylene formation rate on the partial pressure of ethylene. Propylene formation rates on all zeolites are independent of DME partial pressure (Fig. 1). These data are consistent with a mechanism involving a zeolite surface predominantly covered with a DME-derived species that reacts with ethylene to form propylene in the rate-limiting step. Our observations are consistent with the first-order rate dependence in ethylene and zero-order dependence in methanol partial pressure reported by Svelle et al. [26] over H-MFI at 623 K. These authors extrapolated rates to zero conversion because at the higher temperatures used in their study, secondary products were observed; however, under the low temperature and high DME pressure conditions used in this study, no secondary reactions are observed.

Activation barriers and temperature-normalized rate constants were obtained from Arrhenius plots generated from reaction rate data at various temperatures (Fig. 2). Measured rate constants for ethylene methylation show a clear trend from ethylene pressure-dependent studies. (Note: data sets reported in Fig. 1 were obtained at temperatures between 365 and 380 K making direct comparisons possible) and from temperature-dependent studies: $k_{BEA} > k_{MFI} > k_{FER} > k_{MOR}$ (Table 1.) A comparison of the activation energy of H-MFI obtained in this report shows good agreement with previously reported values for reactions of methanol and ethylene at 623 K (94 kJ mol^{-1} compared to 109 kJ mol^{-1}, respectively) [26], and theoretical studies using hybrid MP2/DFT calculations on clusters using corrections from periodic DFT calculations (104 kJ mol^{-1}) [58] and a simplified cluster with a harmonic oscillator approximation for zeolite framework bonds (94 kJ mol^{-1}) [52].

3.2. Propylene methylation

An analogous set of experiments to those conducted for ethylene methylation was performed for propylene methylation over H-MFI, H-BEA, H-FER, and H-MOR zeolites. Reaction rates for butene formation increase linearly with increasing propylene partial pressure and are independent of the DME partial pressure (Fig. 3). Svelle et al. [27] have reported similar trends for propylene and methanol partial pressures for the methylation of propylene to butenes with methanol on H-ZSM-5 at 523 K. We show that first-order dependence in propylene and zero-order dependence in dimethyl ether describe the kinetics of propylene methylation across various zeolites.

A variety of temperatures were required to maintain butene conversions below 0.2% as secondary reactions became significant, particularly on H-BEA. In light of this fact, data shown in the pressure dependence studies are not directly comparable as they were in the case of ethylene methylation. Arrhenius plots generated from propylene methylation rate data at various temperatures show that these catalysts exhibit similar activation energies, but rate constants at 413 K vary by a factor of 30 (Fig. 4 and Table 2). A comparison of the activation energy of H-MFI obtained in this report shows good

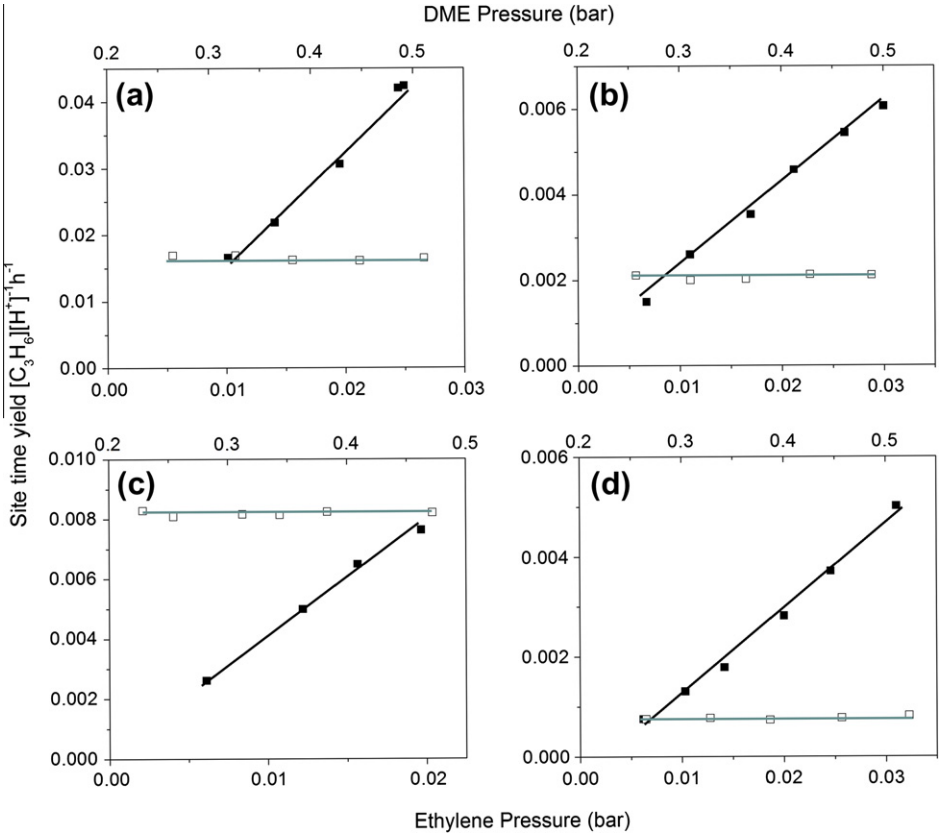

Fig. 1. Dependence of the propylene formation rate on ethylene partial pressure (closed symbols) and DME partial pressure (open symbols). Ethylene pressure was varied from 0.005 to 0.034 bar, and DME pressure was varied from 0.21 to 0.52 bar DME. (a) H-BEA at 365 K (b) H-FER at 370 K (c) H-MFI at 370 K and (d) H-MOR at 380 K.

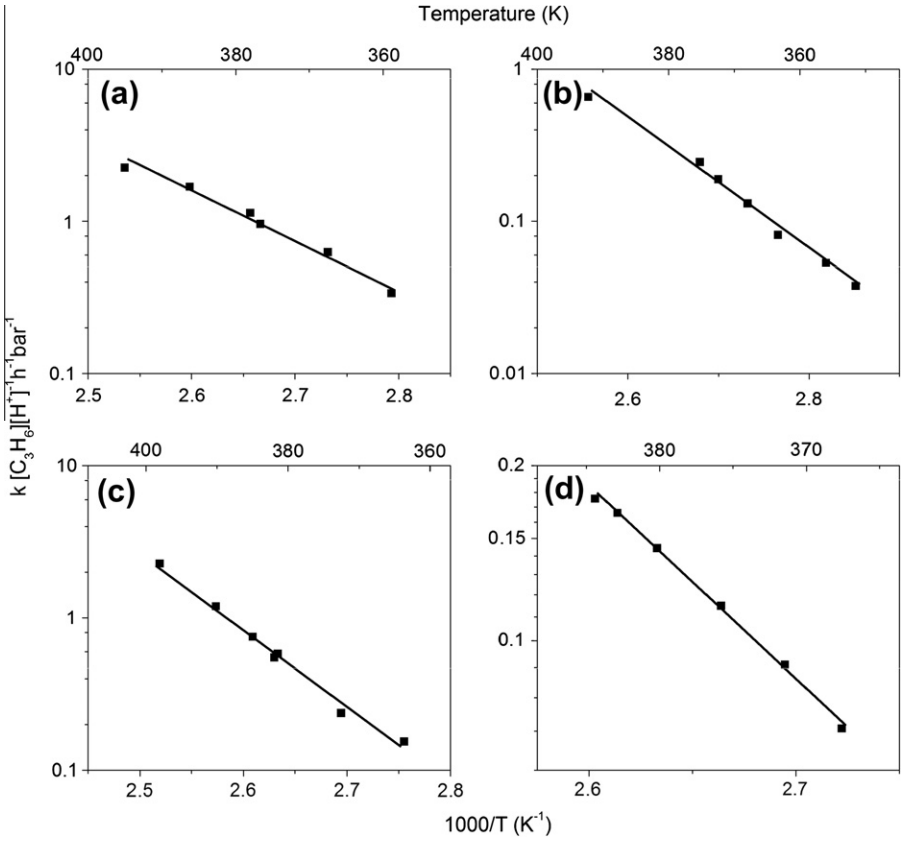

Fig. 2. Temperature dependence of the first-order rate constant for propylene formation in ethylene methylation reactions (0.02 bar C_2H_4 and 0.31 bar DME, T = 360–400 K). (a) H-BEA (b) H-FER (c) H-MFI and (d) H-MOR.

agreement with previously reported values for methylation of propylene at 623 K with methanol (61 kJ mol^{-1} compared to 69 kJ mol^{-1}, respectively) [27], and theoretical studies using hybrid MP2/DFT calculations on clusters using corrections from periodic DFT calculations (64 kJ mol^{-1}) [58] and a simplified cluster with a harmonic oscillator approximation for zeolite framework bonds (62 kJ mol^{-1}) [52]. The reaction rate constant calculated for propylene methylation over H-BEA is within a factor of two compared to the first-order rate constant calculated from the propylene methylation rate reported by Simonetti et al. (1.5×10^{-2} compared to 7.4×10^{-3} mol [mol Al s bar]$^{-1}$ at 473 K) [9].

The pressure dependence studies discussed above show that olefin methylation proceeds via the same mechanism regardless of olefin chain length and zeolite topology, making the comparison of rate constants and activation parameters across these variables valid. Structures MFI and BEA systematically show higher rates of olefin methylation compared to FER and MOR frameworks for both ethylene and propylene, showing that olefin methylation reactions proceed faster over zeolites with three-dimensional connectivity. Our results for olefin methylation kinetics on different zeolites reported in Tables 1 and 2 are in agreement with those reported by Svelle et al. [26,27] for H-ZSM-5 by tracking ^{13}C methanol methylation of C_2–C_4 olefins at 623 K. The data reported in Tables 1 and 2 show that olefin methylation rate constants increase and activation energies decrease systematically for higher-order olefins. These trends are consistent with those expected for carbocation stability with increasing alkyl substitution. Pre-exponential factors observed in this study are upper-bound by those outlined by Dumesic et al. [61] for Eley–Rideal mechanisms on surfaces (<10^{12} h^{-1} bar^{-1}).

Table 1
A comparison of kinetic parameters for ethylene methylation over proton form zeolites.

Sample (Si/Al)	E_a (kJ mol^{-1})	k_{373} (h^{-1} bar^{-1})	A (h^{-1} bar^{-1})
H-FER (10)	84 ± 2	0.21	1×10^{11}
H-MFI (40)	94 ± 3	0.35	3×10^{9}
H-MOR (11)	61 ± 3	0.08	4×10^{7}
H-BEA (12)	62 ± 2	0.79	3×10^{8}

3.3. Mechanism of olefin methylation reactions: co-adsorbed species or surface CH_3 groups

An outstanding question pertaining to the methylation of olefins is the identity of the active DME-derived species on the zeolite surface that is responsible for the methylation of olefins. A brief discussion of literature regarding possible surface species at zeolite Al sites under olefin methylation conditions is provided to rationalize the observed reaction kinetics and isotopomer distributions in our reaction studies. The surface species listed below have been postulated to exist on zeolite Al sites under olefin methylation conditions in the literature:

(i) a co-adsorbed DME/methanol and olefin complex,
(ii) methanol dimers, and
(iii) surface-bound methoxide groups.

In a series of papers, Svelle et al. [51,59] have shown that the heats of co-adsorption for DME/methanol and an olefin are largely influenced by the choice of methylating agent (97 kJ mol^{-1} for DME/C_3H_6 co-adsorption compared to 114 kJ mol^{-1} for methanol/C_3H_6 co-adsorption) and not the olefin (111 kJ mol^{-1} and 114 kJ mol^{-1} for C_2H_4 and C_3H_6, respectively, at 298 K) using com-

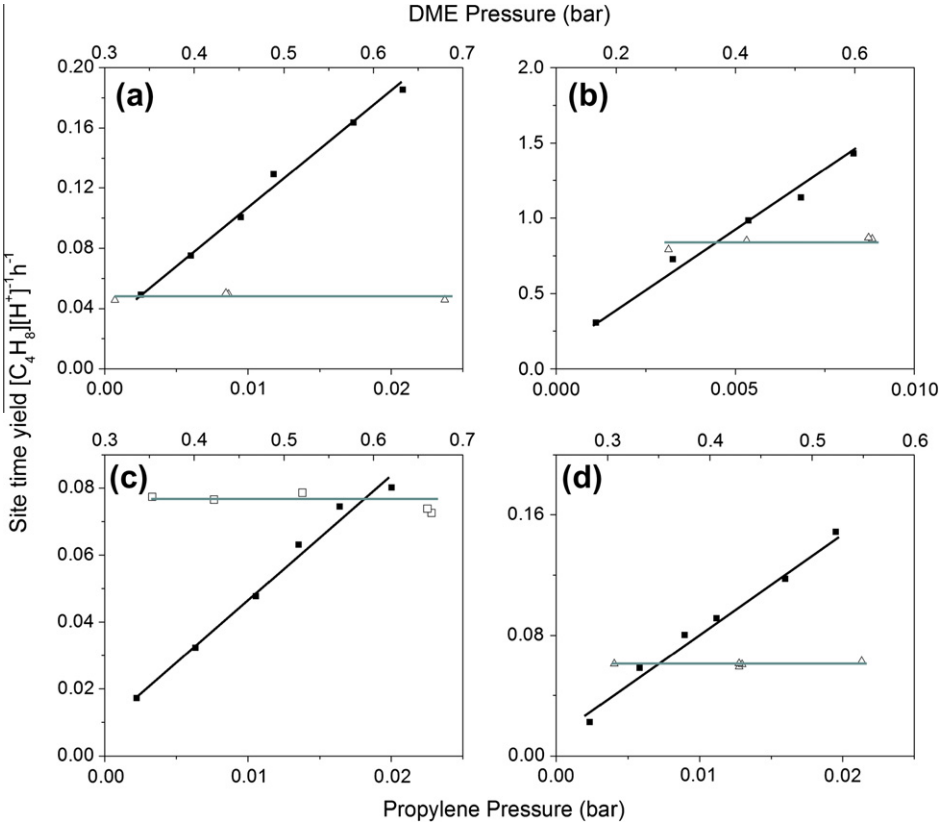

Fig. 3. Dependence of the butene formation rate on propylene partial pressure (closed symbols) and DME partial pressure (open symbols). Propylene pressure was varied from 0.002 to 0.023 bar, and DME pressure was varied from 0.30 to 0.69 bar DME. (a) H-BEA at 355 K, (b) H-MFI at 404 K, (c) H-MOR at 404 K, and (d) H-FER at 420 K.

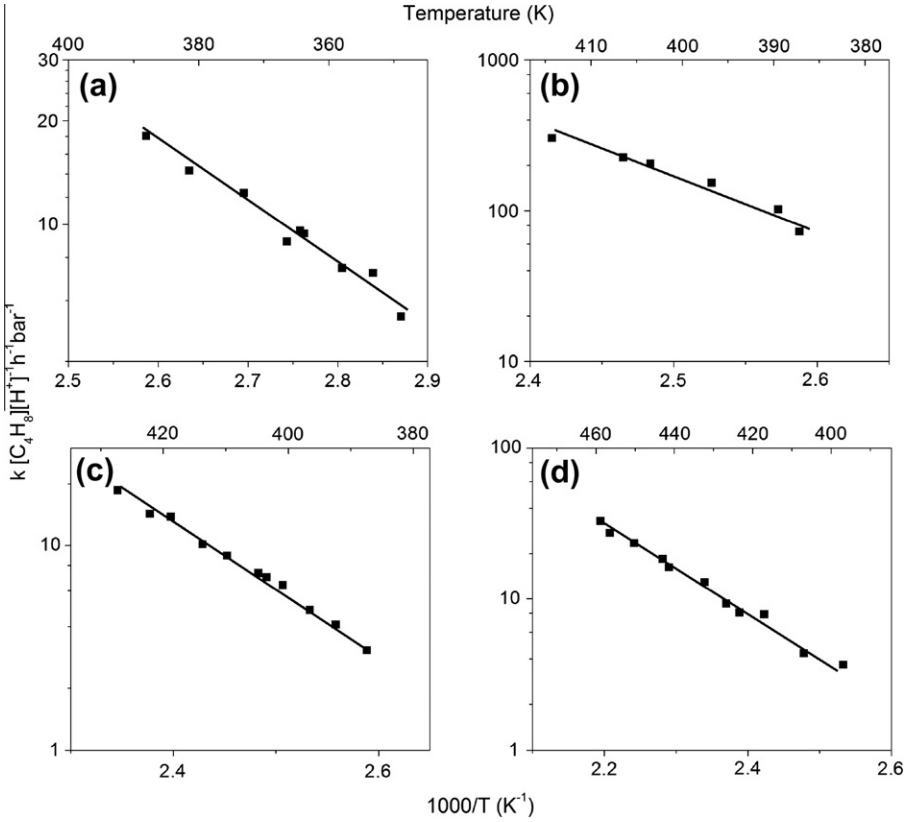

Fig. 4. Temperature dependence of the first-order rate constant for butene formation in propylene methylation reactions (0.01 bar C_3H_6 and 0.62 bar DME, T = 345–430 K). (a) H-BEA, (b) H-MFI, (c) H-MOR, and (d) H-FER.

bined DFT and ab initio calculations on 4T model zeolite clusters. The relative importance of the choice of methylating agent was confirmed experimentally as a 2.5-fold increase in the rate of propylene methylation was observed when feeding DME compared to methanol at 523 K over H-ZSM-5 [59]. Theoretical studies carried out on H-ZSM-5 by Sauer et al. [58] using hybrid MP2/DFT calculations with periodic boundary conditions have also shown that the adsorption of methanol is stronger than that of subsequent co-adsorption with an olefin (−115 for methanol adsorption compared with −37 and −53 kJ mol^{-1} for C_2H_4 and C_3H_6 co-adsorption, respectively) and a ~2 kJ mol^{-1} difference was observed when ethylene was co-adsorbed with methanol in a purely siliceous framework compared to a framework containing Brønsted acid sites, indicating that van der Waals interactions with the zeolite pore walls are the dominant factor in ethylene adsorption as opposed to adsorbing at a Brønsted acid site. Work from Mirth and Lercher [62] shows that toluene/methanol co-adsorption complexes decompose first by loss of toluene at 473 K under 10^{-6} mbar vacuum, followed by the incomplete desorption of methanol using temperature-programmed desorption techniques monitored via infrared spectroscopy and mass spectrometry. These studies clearly show that the major contribution to the heat of adsorption of DME/methanol and olefin co-adsorbed complexes arises from the initial adsorption of the methylating agent.

Maihom et al. [63] have modeled methanol and DME methylation of ethylene using ONIOM hybrid functionals on 4T clusters and concluded that methanol-mediated methylation may be inhibited by the competitive formation of methanol dimers. The formation of alcohol-derived dimer species within zeolite channels has been confirmed in the literature, including the formation of ethanol dimers in dehydration reactions for the formation of diethyl ether [60]. Evidence for methanol dimer formation has been shown by Lee and Gorte based on the observation that the differential heat of adsorption for methanol on H-ZSM-5 (ΔH_{ads} = −115 kJ mol^{-1}) does not change significantly for loadings up to 2 methanol molecules per acid site using microcalorimetry experiments at 400 K [64]. Waroquier et al. [36] have reported an enthalpy of adsorption, ΔH_{ads} = −73.3 kJ mol^{-1}, and an activation barrier, E_{act} = 98 kJ mol^{-1} for the formation of methanol dimers on model H-ZSM-5 at 720 K using ONIOM calculations over 30T and 46T clusters. Methanol activation studies performed by Blaszkowski and van Santen using self-consistent non-local corrected DFT have shown that the adsorption of a single methanol molecule on a Brønsted acid site has a ΔH_{ads} = −75 kJ mol^{-1} and the formation of methanol dimers has an enthalpy of adsorption, ΔH_{ads} = −121–130 kJ mol^{-1} (1T vs. 3T cluster) kJ mol^{-1} [65]. With similar adsorption energies to those reported for methanol-alkene co-adsorbed species (−111–152 for ethylene and −114–168 for propylene) [51,58,59] and observed 2 methanol-per-site loadings from microcalorimetric measurements taken at 400 K [64], the formation of methanol dimer species is not insignificant when considering mechanistic steps from physisorbed states. Work from Stich et al. [66] has shown that the activation of methanol is most facile in the absence of external hydrogen bonding using first-principle molecular dynamics simu-

Table 2
A comparison of kinetic parameters for propylene methylation over proton form zeolites.

Sample (Si/Al)	E_a (kJ mol^{-1})	k_{413} (h^{-1} bar^{-1})	A (h^{-1} bar^{-1})
H-FER (10)	57 ± 2	6.5	1×10^8
H-MFI (40)	61 ± 3	190.2	2×10^{10}
H-MOR (11)	58 ± 4	13.1	3×10^8
H-BEA (12)	54 ± 2	131.2	8×10^{12}

lations. This suggests that methanol dimers would be inadequate methylating agents for olefins as their mutual hydrogen bonding results in enhanced species stability.

Unlike surface-bound higher alkoxides, surface-bound methoxide species are unable to desorb due to the lack of a β-H [34,67]. This results in a highly stable intermediate species, observed via high-temperature *in situ* infrared spectroscopy studies to exist in vacuum at 673 K before surface-bound C–H stretches diminished in coke formation [68]. Bosacek [69] and Wang and Hunger [34] have experimentally observed surface methoxide species on H-ZSM-5 using solid-state ^{13}C MAS NMR at 473 K in vacuum [69] and continuous flow setups [34], and infrared spectroscopy studies have also reported the formation of surface-bound methoxides using deuterated methanol [70]. The reactivity of observed surface-bound methoxide species has been probed using methanol (forming DME), water (forming methanol), and ammonia (forming methylamines) over zeolites H-Y and H-ZSM-5 and zeotype H-SAPO-34 [34]. Theoretical studies utilizing DFT, ab initio, and mixed methods (ONIOM) over small 3T–5T clusters have reported 215 [71], 217 [72], and 223 [36] kJ mol^{-1} barriers toward the dehydration of a physisorbed methanol molecule on a zeolite acid site to form a surface-bound methoxide species and water. It is these high barriers that have led to the conclusion that mechanisms involving methoxide species are unfavorable to those proceeding via associative mechanisms of co-adsorbates. In recent work, Boronat et al. [73] have studied the formation of surface methoxide species on 121–130 atom clusters of MOR from DME and methanol using DFT-D methods. When dispersion interactions within the MOR framework are taken into consideration, intrinsic activation barriers for surface methoxide formation are 39–150 kJ mol^{-1} from DME and methanol precursors, respectively, in 12-membered ring channels. This recent study shows that computational studies done using small clusters result in inordinately high activation barriers for the formation of surface methoxide species [73].

Based on these observations from literature, we performed co-feed DME and d_6 DME experiments at steady-state olefin methylation reaction conditions to provide mechanistic insight regarding the nature of the active surface species and the role of C–H bonds in the rate-determining step. Unreacted DME and d_6 DME scrambling about C–O bond was observed by the presence of a 1.2:1.5:1 distribution of $d_0/d_3/d_6$ isotopic distribution in the product stream. Similar observations were made using a 1:1 d_0/d_6 DME feed in the absence of the MTH reaction (yielding a 1:2:1 $d_0/d_3/d_6$ isotopic distribution) by Haw et al. at 523 K [38]. Significant scrambling about the C–O bond at the reaction conditions reported herein is consistent with fast and reversible formation of surface-bound methoxides occurring during olefin methylation reaction conditions. A co-adsorbed mechanism would only break the DME C–O bond in direct association with an adsorbed olefin. The olefin methylation rate decreased by a factor of 1.3 in the presence of a 1.2:1 d_0/d_6 DME feed compared to purely unlabeled reagents. This observed rate difference is consistent with a positive secondary kinetic isotope effect, indicating the transition from a sp^3 to sp^2 hybridized methyl species in the generation of the activated complex without the cleavage of a C–H bond [74].

From these experimental results, we propose two possible mechanisms that proceed via a planar methyl transition state (Scheme 2). One of these mechanisms postulates the formation of a cyclopropyl cation intermediate (Scheme 2a). These species have been proposed to explain cracking and hydroisomerization selectivity toward branched hydrocarbons and low yields to light olefins in solid acid catalyzed reactions [75–77]. The reaction mechanism may also proceed through the direct addition of a surface-bound methoxide to an olefin, generating the $n+1$ alkoxide (Scheme 2b). Both of these routes would be rate limiting in the methylation step and necessarily exclude the direct breaking of C–H bonds, as this would yield a primary kinetic isotope effect. Increasing rates and decreasing activation energies with increasing carbon substitution can be explained with increasing cyclopropyl [75–77] and carbocation [8,9] stabilization via electron-donating and hyperconjugative effects from alkyl substituents.

The proposed cyclopropyl mechanism explains *in situ* infrared spectroscopic observations by Yamazaki et al. [68] of the selective regeneration of zeolite active sites on H-ZSM-5 from hydrogen originating from methanol/DME in d_3-methanol methylation of olefins, as the cyclopropyl intermediate can only be protonated by the hydrogen-rich surface methoxide group. While the cyclopropyl mechanism explains the experimental results reported herein and the observations by Yamazaki et al. [68], other zeolites may proceed through cyclopropyl or carbocationic intermediates as outlined in Scheme 2.

Our studies in this report show that olefin methylation reactions proceed via similar mechanistic routes on proton-form BEA, MFI, FER, and MOR zeolites; however, these reactions are propagated to varying extents by different zeolites, thereby providing an initial hypothesis for the marked diversity in C_1 homologation selectivity and yield observed with varying structure [78]. Our findings also evidence that surface methoxide groups are formed

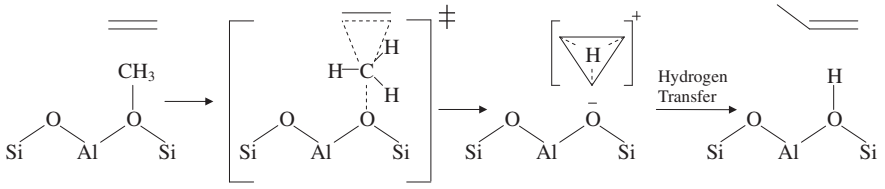

Scheme 2a. Proposed ethylene methylation scheme involving the addition of a surface-bound methoxide group across the olefinic double bond to form a cyclopropyl cation intermediate. Rapid hydrogen transfer, deprotonation, and ring collapse form propylene and regenerate a zeolitic Brønsted acid site.

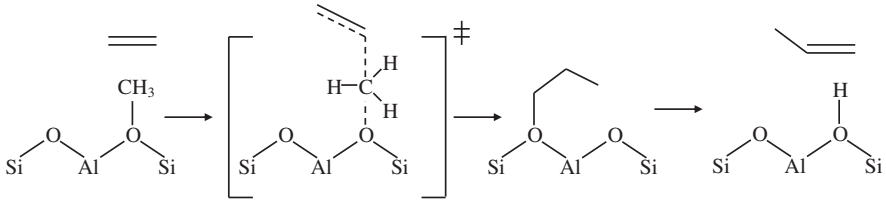

Scheme 2b. Proposed ethylene methylation scheme involving the addition of a surface-bound methoxide group to ethylene to form a propoxide intermediate via a planar CH_3^+ group. Deprotonation at the β-position forms propylene and regenerates a zeolitic Brønsted acid site.

under methylation reaction conditions and that the transition state of the rate-limiting step proceeds via an sp^2 hybridized configuration generated from an sp^3 hybridized precursor state without breaking C–H bonds consistent with these surface-bound methoxide species being responsible for the methylation of olefins.

4. Conclusions

Rate constants for ethylene and propylene methylation over H-MFI, H-BEA, H-MOR, and H-FER at temperatures <473 K in excess DME and ~0.2% conversion have shown that H-BEA and H-MFI propagate the olefin methylation cycle of the hydrocarbon pool mechanism to a greater extent than H-MOR and H-FER. Observed rate constants and activation parameters for H-MFI and H-BEA coincide with those previously reported at higher temperatures and conversions [9,26,27]. Rate constants were found to be systematically higher, and activation energies were found to be systematically lower for C_3H_6 methylation compared to C_2H_4 methylation for every zeolite framework studied, showing that increased olefin substitution affords an increased stabilization of reaction intermediates and/or transition states. Pressure dependence experiments show a first-order rate dependence on olefin partial pressure and a zero-order rate dependence on DME partial pressure over all frameworks studied, consistent with a zeolite surface predominately covered with DME-derived species reacting with an olefin. Temperature dependence studies yielded pre-exponential factors consistent with Eley–Rideal kinetics, also in line with an activated DME-derived surface species reacting with an olefin [61].

Steady-state ethylene methylation in the presence of unlabeled and d_6 DME has shown that the scission and formation of the DME C–O bond is fast compared to olefin methylation reactions through the statistical distribution of $d_0/d_3/d_6$ DME in the unreacted feed, indicating the facile formation of surface methoxide species on the zeolite surface. A secondary kinetic isotope effect was observed with the introduction of d_6 DME into the reaction system, consistent with a planar transition state for the formation of surface methoxide species from a tetrahedral precursor in the absence of C–H/C–D bond cleavage. These experimental observations are consistent with a mechanism for olefin methylation on all zeolites involving the formation of surface methoxide groups that react with olefins.

Acknowledgments

This work was supported by the Abu Dhabi-Minnesota Institute for Research Excellence (ADMIRE); a partnership between the Petroleum Institute of Abu Dhabi and the Department of Chemical Engineering and Materials Science of the University of Minnesota. Acknowledgement is also made to the donors of the American Chemical Society Petroleum Research Fund for partial support of this research (ACS PRF DNI5 49591) and the National Science Foundation (CBET 1055846). The authors would also like to thank Joel Fawaz and Yong Sam Ng for their contributions to the reaction studies presented herein.

Appendix A. Supplementary material

Supplementary data associated with this article can be found, in the online version, at doi:10.1016/j.jcat.2011.09.018.

References

[1] M. Bowker, H. Houghton, K.C. Waugh, J. Chem. Soc., Faraday Trans. 77 (1981) 3023–3036.
[2] M. Bowker, R.A. Hadden, H. Houghton, J.N.K. Hyland, K.C. Waugh, J. Catal. 109 (1988) 263–273.
[3] N.M. Laurendeau, Prog. Energy Combust. Sci. 4 (1978) 221–270.
[4] W.Y. Wen, Catal. Rev. Sci. Eng. 22 (1980) 1–28.
[5] D.A. Hickman, L.D. Schmidt, Science 259 (1993) 343–346.
[6] D. Sutton, B. Kelleher, J.R.H. Ross, Fuel Process. Technol. 73 (2001) 155–173.
[7] M. Asadullah, S. Ito, K. Kunimori, M. Yamada, K. Tomishige, J. Catal. 208 (2002) 255–259.
[8] J.H. Ahn, B. Temel, E. Iglesia, Angew. Chem. Int. Ed. 48 (2009) 3814–3816.
[9] D.A. Simonetti, J.H. Ahn, E. Iglesia, J. Catal. 277 (2011) 173–195.
[10] C.D. Chang, J.C.W. Kuo, W.H. Lang, S.M. Jacob, J.J. Wise, A.J. Silvestri, Ind. Eng. Chem. Process Des. Dev. 17 (1978) 255–260.
[11] I.M. Dahl, S. Kolboe, Catal. Lett. 20 (1993) 329–336.
[12] I.M. Dahl, S. Kolboe, J. Catal. 149 (1994) 458–464.
[13] R.M. Dessau, J. Catal. 99 (1986) 111–116.
[14] J.F. Haw, J.B. Nicholas, W.G. Song, F. Deng, Z.K. Wang, T. Xu, C.S. Heneghan, J. Am. Chem. Soc. 122 (2000) 4763–4775.
[15] D.M. McCann, D. Lesthaeghe, P.W. Kletnieks, D.R. Guenther, M.J. Hayman, V. Van Speybroeck, M. Waroquier, J.F. Haw, Angew. Chem. Int. Ed. 47 (2008) 5179–5182.
[16] U. Olsbye, M. Bjorgen, S. Svelle, K.P. Lillerud, S. Kolboe, Catal. Today 106 (2005) 108–111.
[17] J.F. Haw, W.G. Song, D.M. Marcus, J.B. Nicholas, Accounts Chem. Res. 36 (2003) 317–326.
[18] W.G. Song, D.M. Marcus, H. Fu, J.O. Ehresmann, J.F. Haw, J. Am. Chem. Soc. 124 (2002) 3844–3845.
[19] W.O. Haag, R.M. Lago, P.G. Rodewald, J. Mol. Catal. 17 (1982) 161–169.
[20] C.D. Chang, Catal. Rev. Sci. Eng. 25 (1983) 1–118.
[21] M. Stocker, Microporous Mesoporous Mater. 29 (1999) 3–48.
[22] S.M. Campbell, X.Z. Jiang, R.F. Howe, Microporous Mesoporous Mater. 29 (1999) 91–108.
[23] B. Arstad, S. Kolboe, O. Swang, J. Phys. Chem. B 108 (2004) 2300–2308.
[24] K. Hemelsoet, A. Nollet, M. Vandichel, D. Lesthaeghe, V. Van Speybroeck, M. Waroquier, ChemCatChem 1 (2009) 373–378.
[25] O. Mikkelsen, P.O. Ronning, S. Kolboe, Microporous Mesoporous Mater. 40 (2000) 95–113.
[26] S. Svelle, P.A. Ronning, S. Kolboe, J. Catal. 224 (2004) 115–123.
[27] S. Svelle, P.O. Ronning, U. Olsbye, S. Kolboe, J. Catal. 234 (2005) 385–400.
[28] Z. Cui, Q. Liu, W. Song, L. Wan, Angew. Chem. Int. Ed. 45 (2006) 6512–6515.
[29] Z. Cui, Q. Liu, Z. Ma, S. Bian, W. Song, J. Catal. 258 (2008) 83–86.
[30] C. Wang, Y. Wang, H. Lie, Z. Xie, Z. Liu, J. Catal. 271 (2010) 386–391.
[31] G.A. Olah, Angew. Chem. Int. Ed. 44 (2005) 2636–2639.
[32] G.A. Olah, Catal. Lett. 93 (2004) 1–2.
[33] C.D. Chang, A.J. Silvestri, J. Catal. 47 (1977) 249–259.
[34] W. Wang, M. Hunger, Accounts Chem. Res. 41 (2008) 895–904.
[35] D. Lesthaeghe, V. Van Speybroeck, G.B. Marin, M. Waroquier, Chem. Phys. Lett. 417 (2006) 309–315.
[36] D. Lesthaeghe, V. Van Speybroeck, G.B. Marin, M. Waroquier, Angew. Chem. Int. Ed. 45 (2006) 1714–1719.
[37] D. Lesthaeghe, V. Van Speybroeck, G.B. Marin, M. Waroquier, Ind. Eng. Chem. Res. 46 (2007) 8832–8838.
[38] D.M. Marcus, K.A. McLachlan, M.A. Wildman, J.O. Ehresmann, P.W. Kletnieks, J.F. Haw, Angew. Chem. Int. Ed. 45 (2006) 3133–3136.
[39] R.M. Dessau, R.B. LaPierre, J. Catal. 78 (1982) 136–141.
[40] I.M. Dahl, S. Kolboe, J. Catal. 161 (1996) 304–309.
[41] S. Teketel, U. Olsbye, K. Lillerud, P. Beato, S. Svelle, Microporous Mesoporous Mater. 136 (2010) 33–41.
[42] C. Wang, Y. Wang, Z. Xie, Z. Liu, J. Phys. Chem. C 113 (2009) 4584–4591.
[43] M. Bjorgen, U. Olsbye, D. Petersen, S. Kolboe, J. Catal. 221 (2004) 1–10.
[44] S. Kolboe, S. Svelle, B. Arstad, J. Phys. Chem. A 113 (2009) 917–923.
[45] D. Lesthaeghe, V. Van Speybroeck, M. Waroquier, Phys. Chem. Chem. Phys. 11 (2009) 5222–5226.
[46] W.G. Song, J.F. Haw, J.B. Nicholas, C.S. Heneghan, J. Am. Chem. Soc. 122 (2000) 10726–10727.
[47] D. Lesthaeghe, B. De Sterck, V. Van Speybroeck, G.B. Marin, M. Waroquier, Angew. Chem. Int. Ed. 46 (2007) 1311–1314.
[48] D. Lesthaeghe, A. Horre, M. Waroquier, G.B. Marin, V. Van Speybroeck, Chem. - Eur. J. 15 (2009) 10803–10808.
[49] M. Bjorgen, U. Olsbye, S. Kolboe, J. Catal. 215 (2003) 30–44.
[50] D. Lesthaeghe, J. Van der Mynsbrugge, M. Vandichel, M. Waroquier, V. Van Speybroeck, ChemCatChem 3 (2011) 208–212.
[51] S. Svelle, B. Arstad, S. Kolboe, O. Swang, J. Phys. Chem. B 107 (2003) 9281–9289.
[52] V. Van Speybroeck, J. Van der Mynsbrugge, M. Vandichel, K. Hemelsoet, D. Lesthaeghe, A. Ghysels, G.B. Marin, M. Waroquier, J. Am. Chem. Soc. 133 (2011) 888–899.
[53] M. Bjorgen, S. Svelle, F. Joensen, J. Nerlov, S. Kolboe, F. Bonino, L. Palumbo, S. Bordiga, U. Olsbye, J. Catal. 249 (2007) 195–207.
[54] N.Y. Chen, W.J. Reagan, J. Catal. 59 (1979) 123–129.
[55] B.E. Langner, Appl. Catal. 2 (1982) 289–302.
[56] S. Svelle, F. Joensen, J. Nerlov, U. Olsbye, K. Lillerud, S. Kolboe, M. Bjorgen, J. Am. Chem. Soc. 128 (2006) 14770–14771.
[57] Z. Cui, Q. Liu, S. Baint, Z. Ma, W. Song, J. Phys. Chem. C 112 (2008) 2685–2688.
[58] S. Svelle, C. Tuma, X. Rozanska, T. Kerber, J. Sauer, J. Am. Chem. Soc. 131 (2009) 816–825.
[59] S. Svelle, S. Kolboe, O. Swang, U. Olsbye, J. Phys. Chem. B 109 (2005) 12874–12878.
[60] H. Chiang, A. Bhan, J. Catal. 271 (2010) 251–261.

[61] J.A. Dumesic, D.F. Rudd, L.M. Aparicio, J.E. Rekoske, A.A. Trevino, in: The Microkinetics of Heterogeneous Catalysis, American Chemical Society, Washington D.C., 1993, p. 315.
[62] G. Mirth, J.A. Lercher, J. Phys. Chem. 95 (1991) 3736–3740.
[63] T. Maihom, B. Boekfa, J. Sirijaraensre, T. Nanok, M. Probst, J. Limtrakul, J. Phys. Chem. C 113 (2009) 6654–6662.
[64] C.C. Lee, R.J. Gorte, W.E. Farneth, J. Phys. Chem. B 101 (1997) 3811–3817.
[65] S.R. Blaszkowski, R.A. van Santen, J. Phys. Chem. B 101 (1997) 2292–2305.
[66] I. Stich, J.D. Gale, K. Terakura, M.C. Payne, J. Am. Chem. Soc. 121 (1999) 3292–3302.
[67] P. Cheung, A. Bhan, G.J. Sunley, D.J. Law, E. Iglesia, J. Catal. 245 (2007) 110–123.
[68] H. Yamazaki, H. Shima, H. Imai, T. Yokoi, T. Tatsumi, J.N. Kondo, Angew. Chem. Int. Ed. 50 (2011) 1853–1856.
[69] V. Bosacek, J. Phys. Chem. 97 (1993) 10732–10737.
[70] Y. Ono, T. Mori, J. Chem. Soc., Faraday Trans. 77 (1981) 2209–2221.
[71] S.R. Blaszkowski, R.A. van Santen, J. Am. Chem. Soc. 118 (1996) 5152–5153.
[72] C.M. Zicovich-Wilson, P. Viruela, A. Corma, J. Phys. Chem. 99 (1995) 13224–13231.
[73] M. Boronat, C. Martinez, A. Corma, Phys. Chem. Chem. Phys. 13 (2011) 2603–2612.
[74] J.A. Streitwieser, R.H. Jagow Jr., R.C. Fahey, S. Suzuki, J. Am. Chem. Soc. 80 (1958) 2326.
[75] S.T. Sie, Ind. Eng. Chem. Res. 32 (1993) 397–402.
[76] S.T. Sie, Ind. Eng. Chem. Res. 32 (1993) 403–408.
[77] S.T. Sie, Ind. Eng. Chem. Res. 31 (1992) 1881–1889.
[78] T. Mokrani, M. Scurrell, Catal. Rev. 51 (2009) 1–145.